Supplemental Materials

"New insights into band inversion and topological phase of TiNI monolayer"

Shahram Yalameha [1], Zahra Nourbakhsh [1], Mohammad Saeed Bahramy [2], and Daryoosh Vashaee [3,4,*]

[1]*Faculty of Physics, University of Isfahan, 81746-73441, Isfahan, Iran*
[2]*Department of Physics and Astronomy, University of Manchester, Oxford Road, Manchester M13 9PL, UK.*
[3]*Department of Electrical and Computer Engineering, North Carolina State University, Raleigh, NC 27606, USA*
[4]*Department of Materials Science and Engineering, North Carolina State University, Raleigh, NC 27606, USA*

Basic concepts of band inversion

There are several ways we can define the concept of the band structure. The standard way is in terms of *energies;* we solve the Schrödinger equation of solids from the first principles (ab initio) to get both eigenstates and eigenvalues. The eigenvalues will form dense packages that span an energy window (i.e., band theory). If we label the energies by the corresponding wave vector $\boldsymbol{k}$ of the Bloch wavefunction, we can define bands as a function of $\boldsymbol{k}$, $E_n(\boldsymbol{k})$, where n is the band index. Considering the *symmetry* of the crystal, one can define the concept of the band differently. One can define a band by a vector containing the irreducible representations of the Bloch wavefunctions across the BZ. This is the definition of band representation. It should be noted that this is a global description of the band in reciprocal space, and thus, the Bloch wavefunction is not a well-suited basis to describe it. Instead, describing it in terms of localized orbitals in real space (i.e., Wannier functions) is preferred. This concept has led to the theory of topological quantum chemistry (TQC), which can be used to identify the topology of bands in materials. In this theory, the classification of topological materials is formulated by the elementary band representations

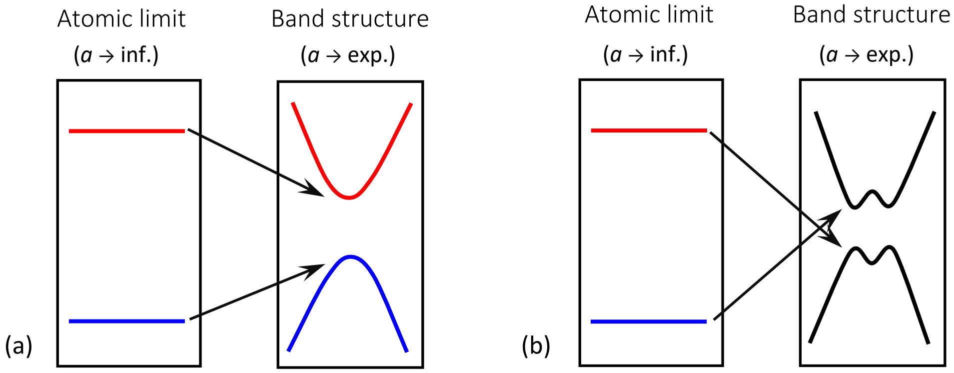

Fig. S1. Schematic of band structure and atomic limit. The atomic limit (lattice constant to infinity) results in many unbound atoms. As the lattice constant approaches the experimental value, the atomic orbitals become Bloch bands where they gain energy dispersion as a function of the Bloch momentum. **(a)** Normal band insulator: the orbital-resolved electronic energy states of the valence band will always remain lower than that of the conduction band at all $\boldsymbol{k}$-points throughout the BZ. **(b)** Nontrivial band insulator: the relative energy positions of the CB (red color) and VB (blue color) are reversed with respect to their atomic limit.

---

[*] Email: dvashae@ncsu.edu

and connectivity graphs (see Ref. [1] for more details). However, in the continuation of this section, we will use the first concept and examine the band inversion and the topology of the bands.

According to band theory, an insulator material is described by a set of filled electronic bands, *i.e.*, valence bands, separated from an empty set of bands, *i.e.*, conduction bands, by an energy gap. Although insulators can have different bandgap values, all the known normal band insulators belong to the same topologically trivial phase as the vacuum (from a topological point of view). This statement can be conceptualized by taking a conventional insulator and adiabatically changing its Hamiltonian (through external parameters) to the atomic limit. Note that the atomic limit means that the lattice constant (a) increases infinitely, leading to several unbound atoms. This process can be viewed as merely changing the energy gap value at each k-point without closing the energy gap. Such a process does not occur for TI. Therefore, these materials, which are not topologically equivalent to vacuum, are the intriguing topological phases of matter. In other words, an insulator is topologically nontrivial if it cannot be continued to any *atomic limit* without either closing a gap or breaking a symmetry [1].

The above conceptual process inspires a definition for *band inversion*. In general, band inversion is a phenomenon in the electronic band structure where the relative energy positions

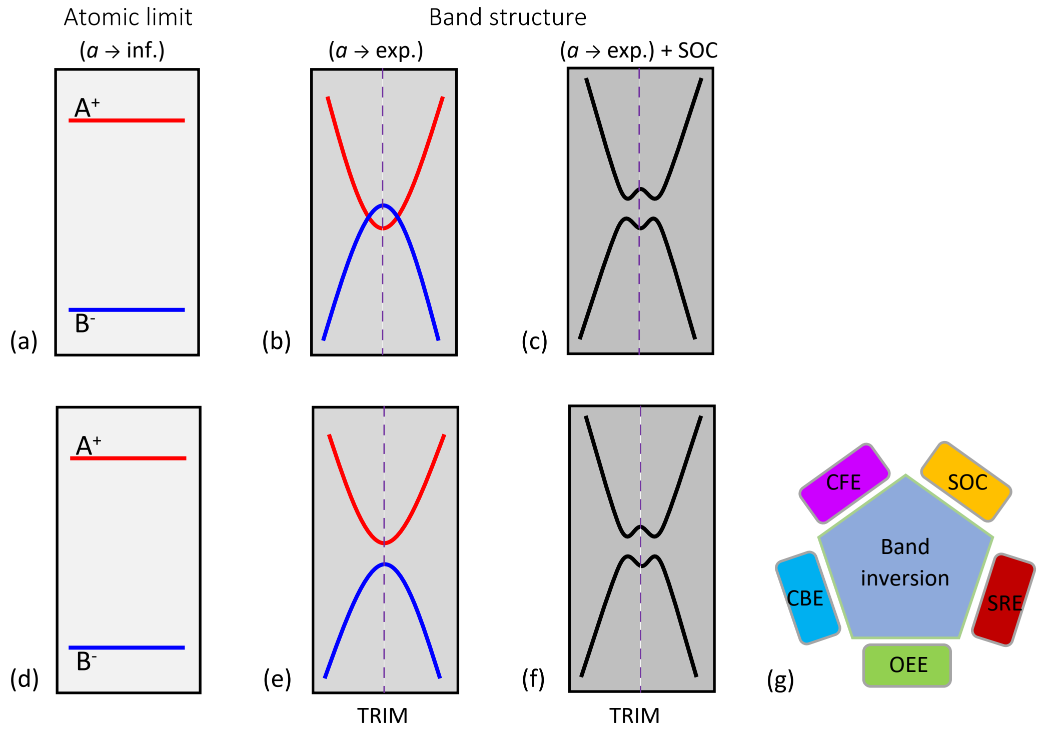

Fig. S2. Schematic of atomic limit and band structure with/without spin-orbit coupling (SOC). **(a-c)** In the A^+B^- material, the VB and CB gain energy dispersion such that these two bands cross at certain TRIM points. When applying the SOC, an energy gap opens. **(d-f)** In this case, in the absence of SOC, there is no band crossing, and the SOC is responsible for both inverting the bands and opening the bandgap. **(g)** Mechanisms of band inversion occurrence. In addition to SOC, there are other inherent causes for band inversion. The scalar relativistic effect (SRE), crystal field effect (CFE), and chemical bonding effect (CBE) are among these effects that can lead directly or indirectly through the SOC to band inversion. There are other external effects (OEE) that can affect the occurrence of band inversions, such as pressure, stress, or impurities.

between the conduction bands (CB) and valence (VB) bands in a solid are reversed with respect to those in its *atomic limit.* Therefore, any nontrivial topological material should have a finite number of band inversions because those that do not can be adiabatically tuned into their atomic limit without closing the gap. Many unbound atoms or ions will result if we consider an insulator and increase the lattice constant to infinity. Now gradually change the lattice constant from infinity to the experimental value. Each atomic level will form a Bloch band and gain dispersion as a function of Bloch-momentum (***k***). For a normal band insulator, the orbital-resolved electronic energy states (OREES) of VB will always remain lower than that of the OREES of CB at all ***k***-points throughout the BZ (Fig. S1(a)). As a result, a normal band insulator is topologically trivial. On the other hand, the OREES of VB energy becomes higher for a topological insulator than OREES of CB at some *k*-points (Fig. S1(b)). Hence, to restore the relative energy order between VB and CB as in the *atomic limit*, one has to close the bulk bandgap, which involves a quantum (topological) phase transition demonstrating the topological inequality between a topological insulator and the vacuum (*atomic limit*). Band inversion indicates that the material has been transferred to the topological phase but does not indicate to which topological class it has passed. Therefore, a topological phase is defined by the topological numbers or topological invariants calculated using the electronic wave function throughout the BZ. In fact, if a system has non-zero band inversions, one still needs to evaluate the topological invariants of the system to determine its topological nontriviality.

Now, if other intrinsic effects are considered, it can be seen that such effects will lead to band inversion at a stage when the lattice constant approaches the experimental value. One of these effects is SOC. Hence, let us imagine a compound like $A^{+}B^{-}$. We label the lowest valence and conduction bands as B^{-} and A^{+}, respectively, as shown in Fig. S2(a). As we tune the lattice constant to the experimental value, the valence and conduction bands gain energy dispersion such that these two bands cross at a certain TRIM point, as shown in Fig. S2(b). In this case, in the vicinity of the TRIM point, where band-crossing occurs, the system gains energy to transfer the electron in the *B* atom back to the *A* atom. It is noteworthy that as the conduction and valence bands cross, they become degenerate at certain *k* points in the BZ. When the SOC is considered, it causes the crossing bands to hybridize and open a global bandgap (Fig. S2(c)). Therefore, the spin-orbit coupling is responsible only for opening the bandgap, and the band inversion has taken place before considering the SOC (see Fig. S2(b)). SnTe is a well-known example of this kind, where a band inversion between the Sn-*p* and Te-*p* orbitals is found even without including the SOC [2].

Now consider another case with a slight difference, as shown in Figs. S2(d-f). Before considering the SOC, no band crossing exists. After considering the SOC, both band inversion and opening of the insulating gap happen. Bi_2Se_3 is an example of this kind [3].

In addition to SOC, other inherent effects, such as the scalar relativistic effect (SRE), crystal field effect (CFE), and chemical bonding effect (CBE), are among the effects that can lead to band inversion directly or indirectly [4-6]. Besides, other external effects (OEE), such as pressure, stress, or impurities, can also lead to band inversion [5, 7, 8]. Depending on the material structure and its dimensions, each effect can help achieve a band inversion (see Fig. S2(g)). Thus, although band inversion cannot define any topological class rigorously, it is very suggestive of identifying novel topological materials for topological class and understanding the topological nature.

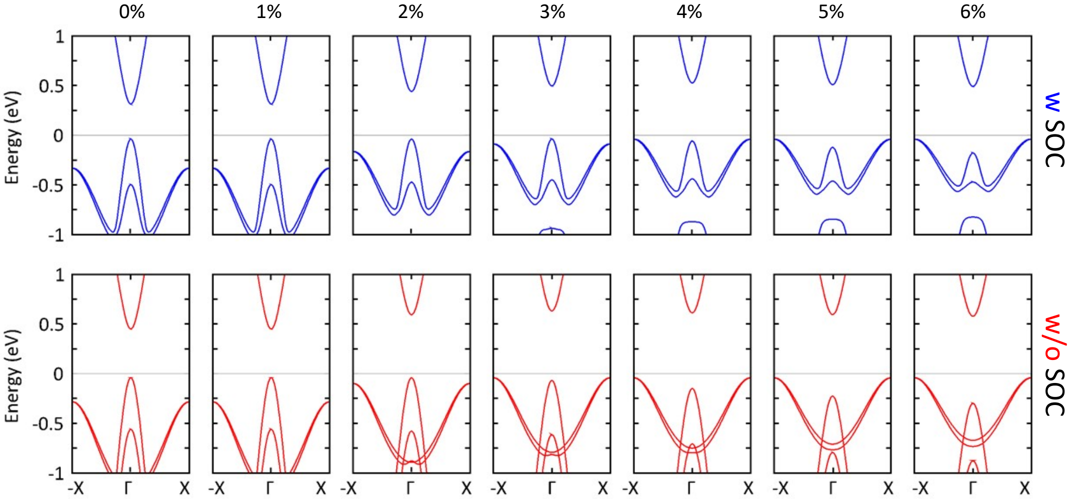

Fig. S3. Band structures of the TiNI monolayer within HSE06 approach under different external uniaxial tension strain along *x*-axis strain without and with SOC.

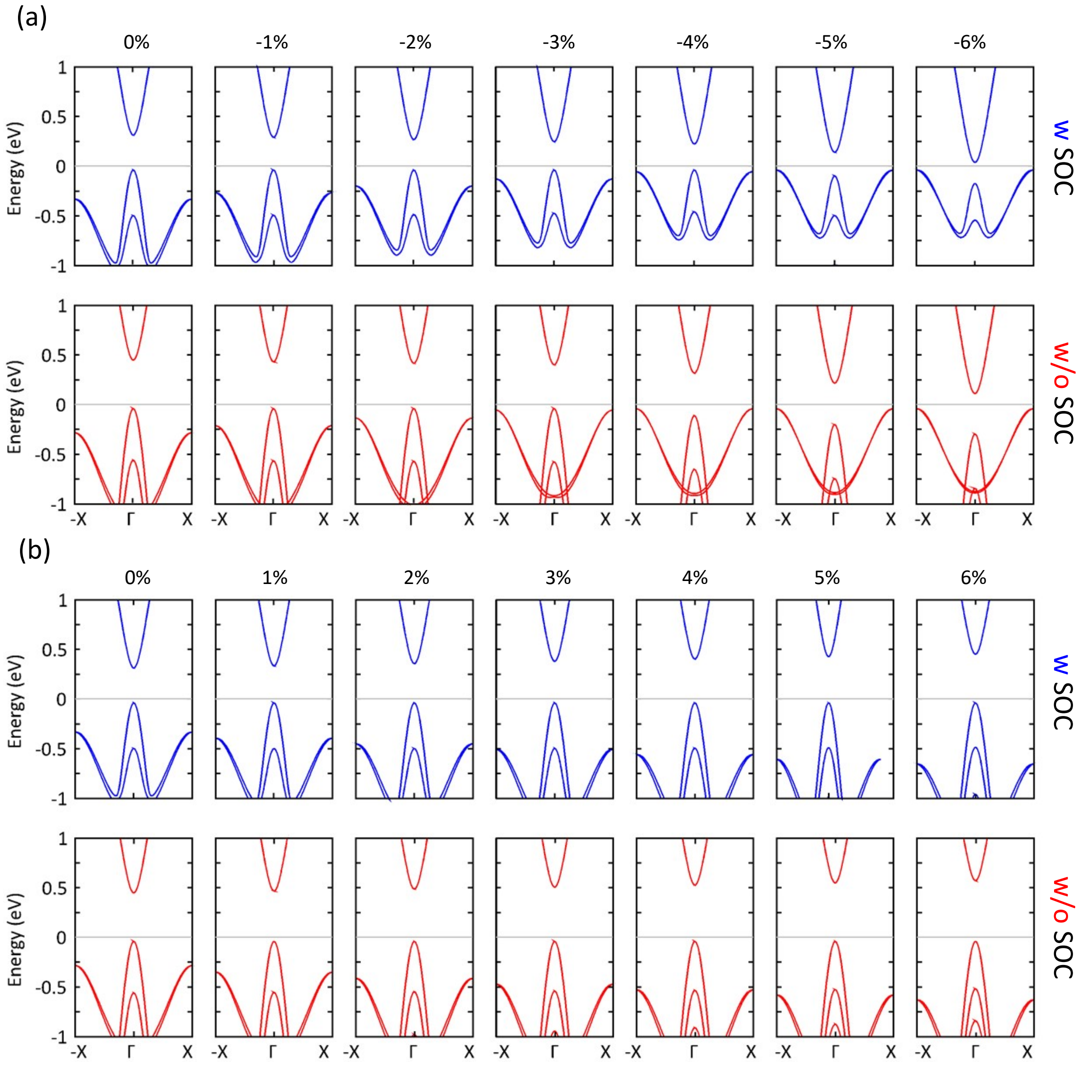

Fig. S4. Band structures of the TiNI monolayer within HSE06 approach under different external uniaxial **(a)** compression and **(b)** tension strains along the *y*-axis without and with SOC.

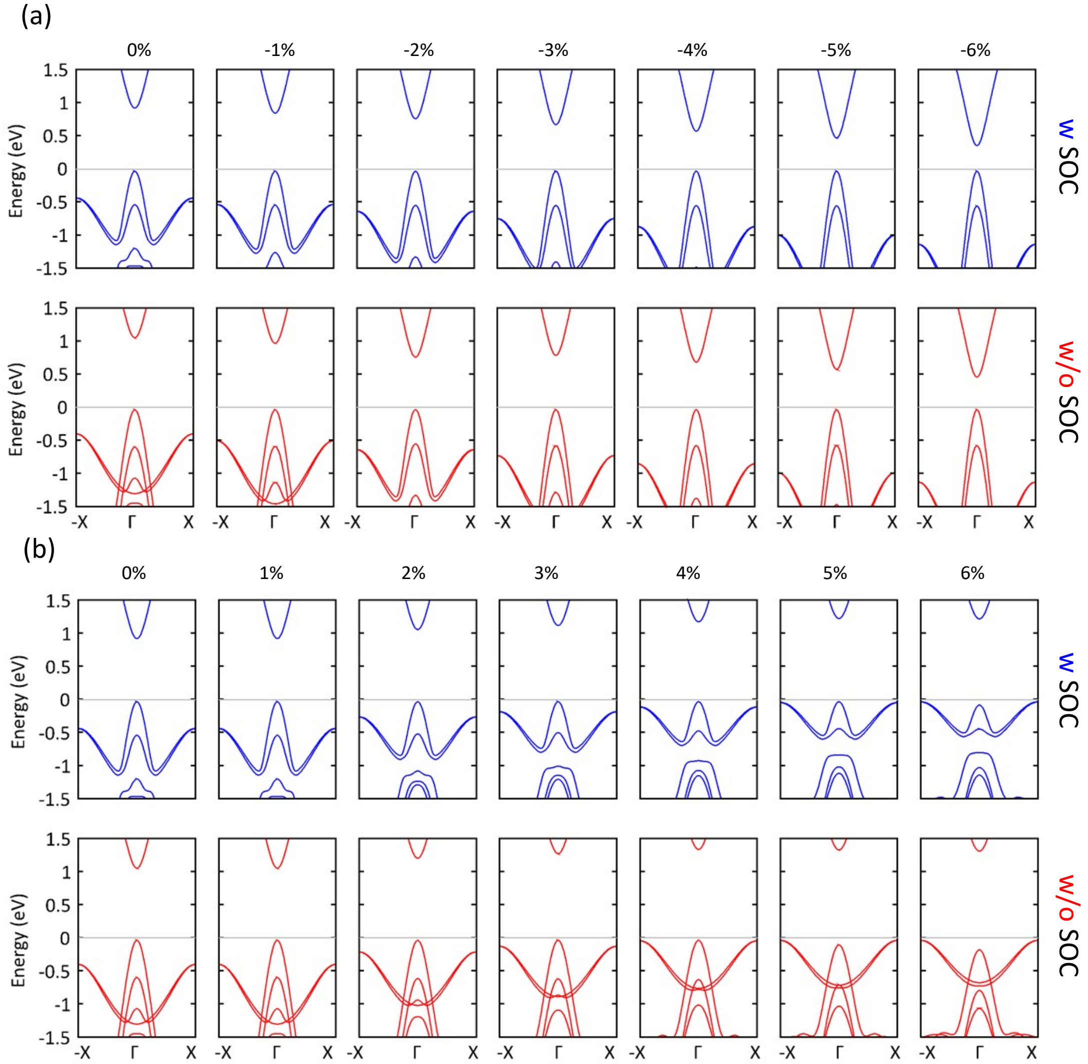

Fig. S5. Band structures of the TiNI monolayer within the PBE0 approach under different external uniaxial **(a)** compression and **(b)** tension strains along the *x*-axis without and with SOC.

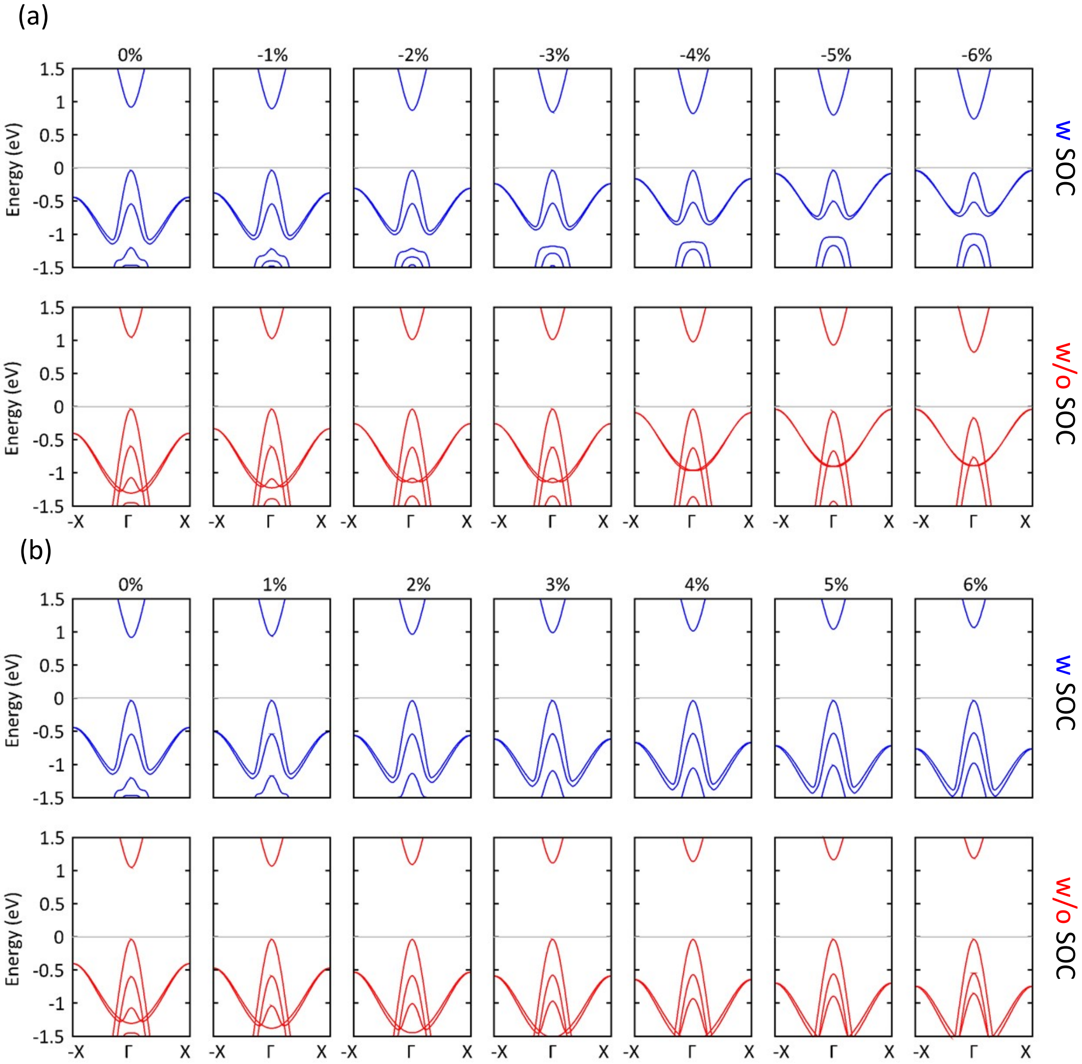

Fig. S6. Band structures of the TiNI monolayer within the PBE0 approach under different external uniaxial **(a)** compression and **(b)** tension strains along the *y*-axis without and with SOC.

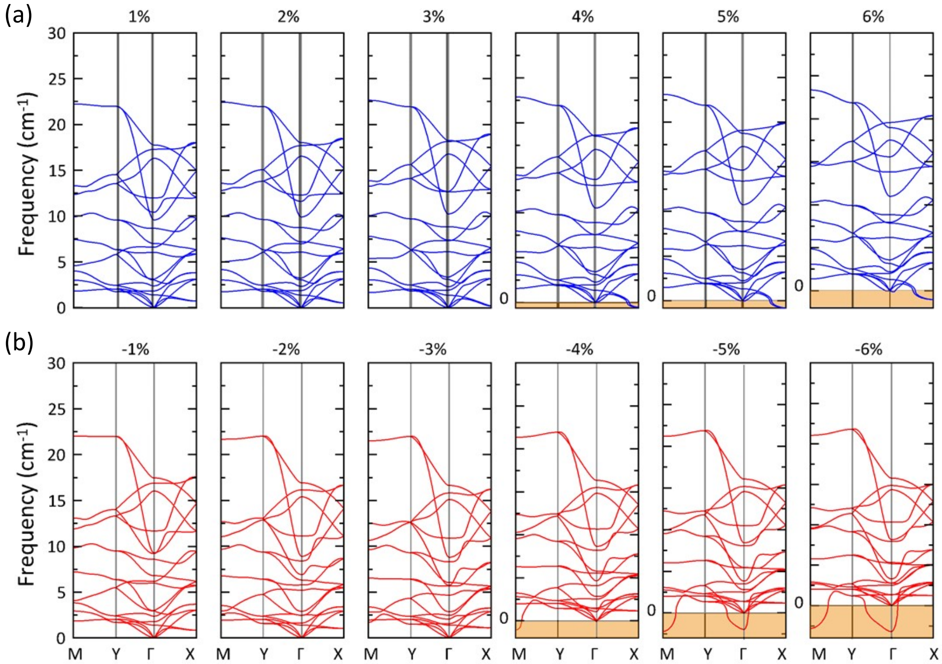

Fig. S7. Phonon dispersion of TiNI monolayer under different external uniaxial **(a)** tension and **(b)** compression strains along the *x*-axis.

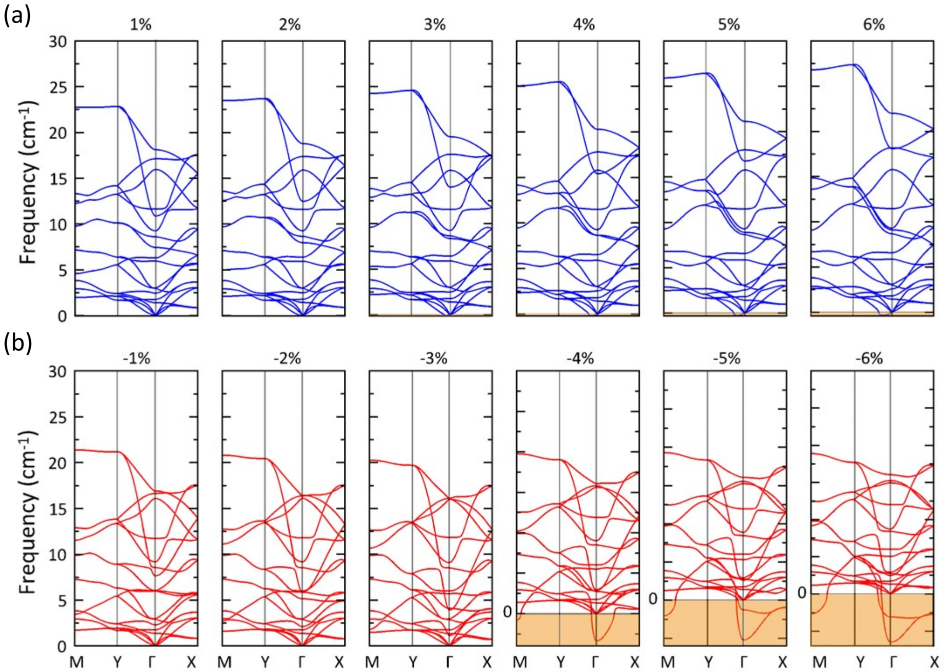

Fig. S8. Phonon dispersion of TiNI monolayer under different external uniaxial **(a)** tension and **(b)** compression strains along the *y*-axis.

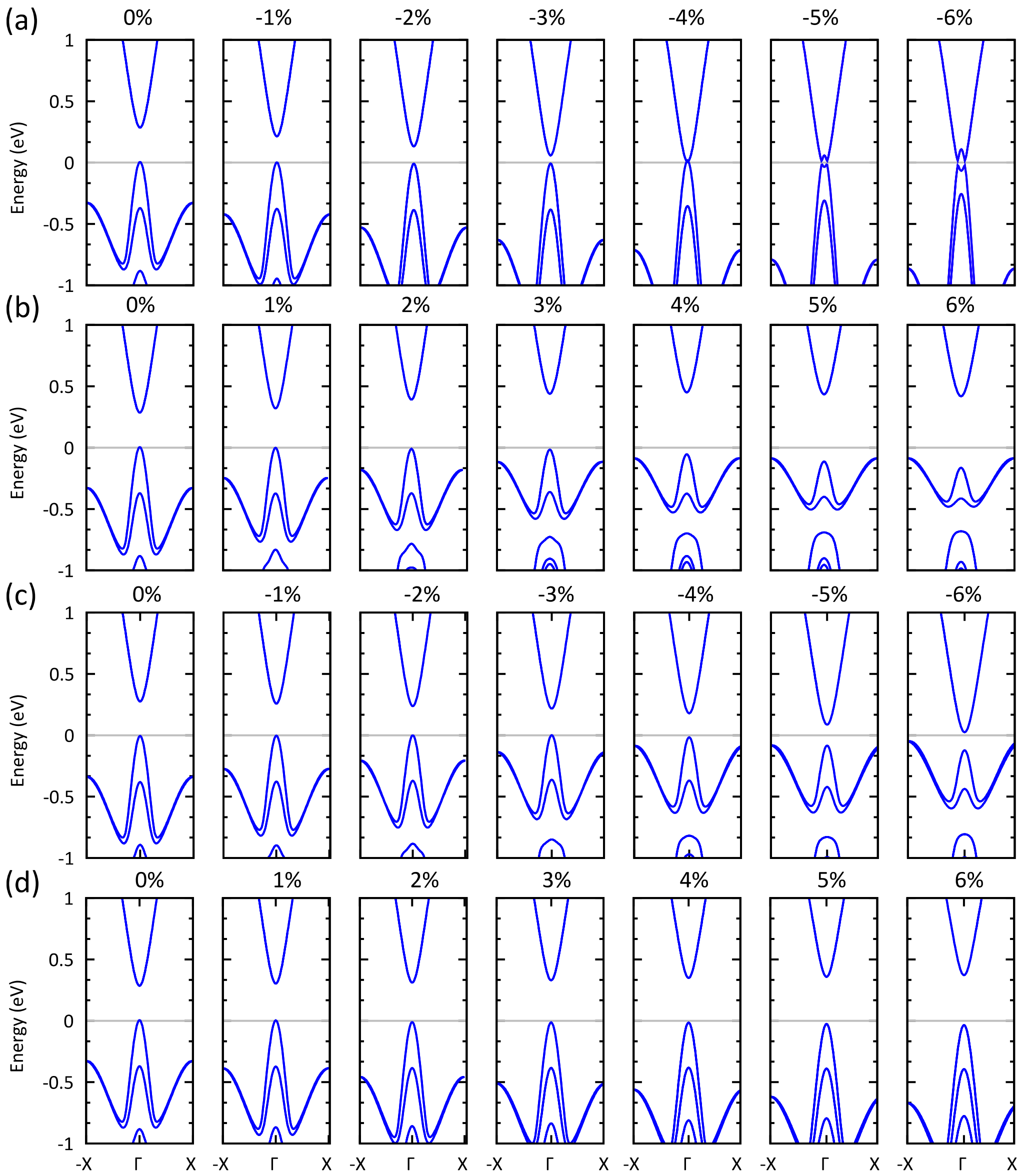

Fig. S9. Band structures of the TiNI monolayer within the TB-mBJ approach under different external uniaxial compression strains along the **(a)** *x*-axis and **(b)** *y*-axis and **(b)** tension strains along the **(c)** *x*-axis and **(d)** *y*-axis with SOC.

References

1. B. Bradlyn, L. Elcoro, J. Cano, M. Vergniory, Z. Wang, C. Felser, M. I. Aroyo, and B. A. Bernevig, "Topological quantum chemistry," Nature **547**, 298-305 (2017).
2. T. H. Hsieh, H. Lin, J. Liu, W. Duan, A. Bansil, and L. Fu, "Topological crystalline insulators in the SnTe material class," Nature communications **3**, 1-7 (2012).
3. H. Zhang, C.-X. Liu, X.-L. Qi, X. Dai, Z. Fang, and S.-C. Zhang, "Topological insulators in Bi 2 Se 3, Bi 2 Te 3 and Sb 2 Te 3 with a single Dirac cone on the surface," Nature physics **5**, 438-442 (2009).
4. Y. Li, S. Chen, K. Hu, X. Wen, P. Zhou, and L. Sun, "Two dimensional topological insulators in bilayer BiB," Computational Materials Science **160**, 82-85 (2019).
5. S. Yalameha, Z. Nourbakhsh, and A. Vaez, "Hydrostatic strain-induced topological phase of KNa2Sb," Journal of Magnetism and Magnetic Materials **468**, 279-286 (2018).
6. Y. Nie, J. Zhang, W. Chen, Q. Xia, X. Wang, and G.-h. Guo, "First-principles design of a Dirac semimetal: An NP monolayer," Physical Review B **101**, 235443 (2020).
7. P. Saeidi, S. Yalameha, and Z. Nourbakhsh, "The investigation of structural, electronic, elastic and thermodynamic properties of Gd1− xYxAuPb alloys: A first principle study," Physics Letters A **383**, 221-230 (2019).
8. S. Chege, P. Ning'i, J. Sifuna, and G. O. Amolo, "Origin of band inversion in topological Bi2Se3," AIP Advances **10**, 095018 (2020).